J. Mt. Sci. (2009) 6: 14–24
DOI 10.1007/s11629-009-0206-4

Drainage Network and Lineament Analysis: An Approach for Potwar Plateau (Northern Pakistan)

Faisal SHAHZAD*, Syed Amer MAHMOOD and Richard GLOAGUEN

Remote Sensing Group, Institute of Geology, Freiberg University of Mining and Technology, Freiberg, 09599, Germany.

**Corresponding Author: geoquaidian@gmail.com*

Abstract: Drainage responds rapidly to tectonic changes and thus it is a potential parameter for tectonogeomorphological analysis. Drainage network of Potwar is a good geological record of movement, displacements, regional uplifts and erosion of the tectonic units. This study focuses on utilizing drainage network extracted from Shuttle Radar Digital Elevation Data (SRTM-DEM) in order to constrain the structure of the Potwar Plateau. SWAN syncline divides Potwar into northern Potwar deformed zone (NPDZ) and southern Potwar platform zone (SPPZ). We extracted the drainage network from DEM and analyzed 112 streams using stream power law. Spatial distribution of concavity and steepness indices were used to prepare uplift rate map for the area. DEM was further utilized to extract lineaments to study the mutual relationship between lineaments and drainage patterns. We compared the local correlation between the extracted lineaments and drainage network of the area that gives us quantitative information and shows promising prospects. The streams in the NPDZ indicate high steepness values as compared to the streams in the SPPZ. The spatial distribution of geomorphic parameters and uplift rates suggest the distinctive deformation among eastern, central and western parts. The local correlation between drainage network and lineaments from DEM is strongly positive in the area within 1 km of radius.

Keywords: Drainage network; lineaments; stream profile analysis; uplift rate; local correlation

Received: 10 July 2008
Accepted: 8 October 2008

Introduction

The Potwar Plateau is a part of North Western Himalayan Fold and thrust belt, and it lies on the western flank of India-Eurasia collision zone. The tectonic settings of the Potwar Plateau are influenced by the northward subduction of the Indian plate beneath Eurasian plate as shown in Figure 1. We used the Digital Elevation Models from SRTM (90 m resolution version 3.0). The drainage networks in active regions are strongly and rapidly influenced due to tectonic and erosion changes, and thus they are potential instruments for tectonogeomorphological analysis. The drainage network of Potwar has preserved good geological record of the movement, displacement, regional uplifts and erosion of tectonic units. The Swan River bisects the Potwar Plateau diagonally and controls its drainage pattern. It divides the Potwar Plateau into northern Potwar deformed zone (NPDZ) and southern Potwar platform zone (SPPZ) on the basis of crustal deformation.

We prepared MATLAB script files to extract drainage network and lineaments from DEM. These scripts took elevation information from DEM and applied D8 Algorithm which calculates flow direction at each cell to the lowest neighboring cells (O'Callaghan and Mark 1984). The vectorization of the flow directions allowed us to calculate stream paths. The extracted drainage network consisted of 112 streams with elevation and upstream area information as a function of spatial locations. We analyzed these individually extracted stream profiles and thus the whole drainage network by using stream power law of scaling relation. The stream profile analysis helped us to calculate geomorphic indices and uplift rates of each stream under certain assumptions. The streams in NPDZ indicated high steepness and concavity indices as compared to the streams in SPPZ. Spatial distribution of geomorphic indices and uplift rates differentiated among eastern, central and western parts. The eastern part showed more deformation and high uplift rates.

The orientation of lineaments and drainage patterns were helpful to calculate the amount of deformation mathematically. We calculated the local correlation between drainage network and lineaments for this propose. This local correlation showed the influence of lineaments on nearby streams and is strongly positive in the area within 1 km radius, i.e., the lineaments within 1 km radius of any stream strongly influence their presence.

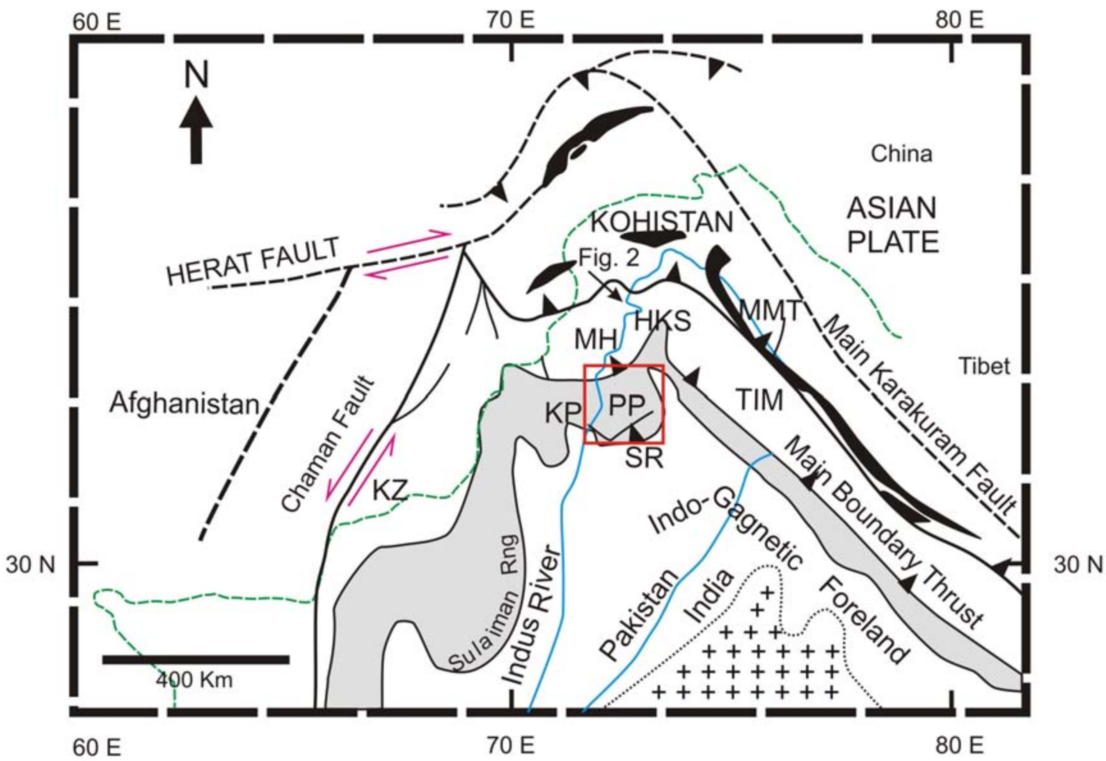

Figure 1 Generalized tectonic map of India-Eurasia collision zone (Pivnik and Wells 1996). The study area is represented by red rectangle and shown in Figure2. PP: the Potwar Plateau; KP: Kohat Plateau; MMT: Main Mantle Thrust; HKS: Hazara Kashmir Syntaxis. Green dashed line represents geographical boundary of Pakistan with China and Afghanistan.

1 Tectonic Settings of the Area

The collisional zones are important for the formation of fold and thrust belts. The Himalayan fold and thrust belt was produced due to the thrusting of the Indian plate beneath the Eurasian plate during Himalayan orogeny. This orogeny consists of Main Karakoram Thrust (MKT), i.e., Shyok Suture zone, Main Mantle Thrust (MMT), i.e., Indus Suture zone, Main Central Thrust (MCT), Main Boundary Thrust (MBT) and Salt Range Thrust (SRT) as major tectonic boundaries. Due to this continuous orogenic process the stress started shifting towards the Main Central Thrust (MCT) and Main Boundary Thrust (MBT), respectively. The northwestern part of this mountain belt refers as northwestern Himalayan fold and thrust belt (NWHFTB), and is shown in Figure 2. The NWHFTB consists of the terrain from MMT to SRT, while Hazara Kashmir Syntaxes and Nanga Parbat Haramosh Massif mark its eastern boundary. The western limit of this fold and thrust belt is marked by some thrust faults in the eastern Afghanistan. This area consists of thin skinned tectonic features of Eocene time (Baker et al. 1988, Jadoon and Frisch 1997, Jadoon et al. 1997, Jan et al. 2005, Kazmi and Jan. 1997, Khan et al. 1986, Monalisa et al. 2002, Monalisa et al. 2007).

The Potwar Plateau is structurally complex and seismically less active part of NWHFTB. It extends from the Main Boundary Thrust (MBT) in the north to the Salt Range Thrust in the south, while the Jehlum Fault and Kalabagh Fault mark their eastern and western boundaries, respectively. This plateau contains surface representation of most of the subsurface structures which help us to study them with remote sensing technology. But in most of the cases, the surface features do not reflect the subsurface structure due to structural complexity. The structural complexity of the area is well distributed in eastern, middle and western section (Jadoon et al. 1997, Moghal et al. 2003, Monalisa et al. 2002).

Active features like Mangla and Maira faults of approximately 10 km long each are present in eastern section. They are WNW-ESE or ENE-WSW trending faults with only dip slip movement recorded along the traces. The short irregular active fault traces of the Jehlum Fault trending NE-SW are also present along the eastern margin of Salt Range. Khairi Murat Fault is another prominent feature in this region. These faults are easily identified with fault scarp. The presence of dislocated Pleistocene river terraces and fan surfaces forms distinctive fault scarplets (Nakata et al. 1991). This area consists of steeply dipping active faults which produce straight traces that clearly offset geomorphic features. The tectonic map of the Potwar Plateau is shown in Figure 2 and different localized faults are also mentioned here.

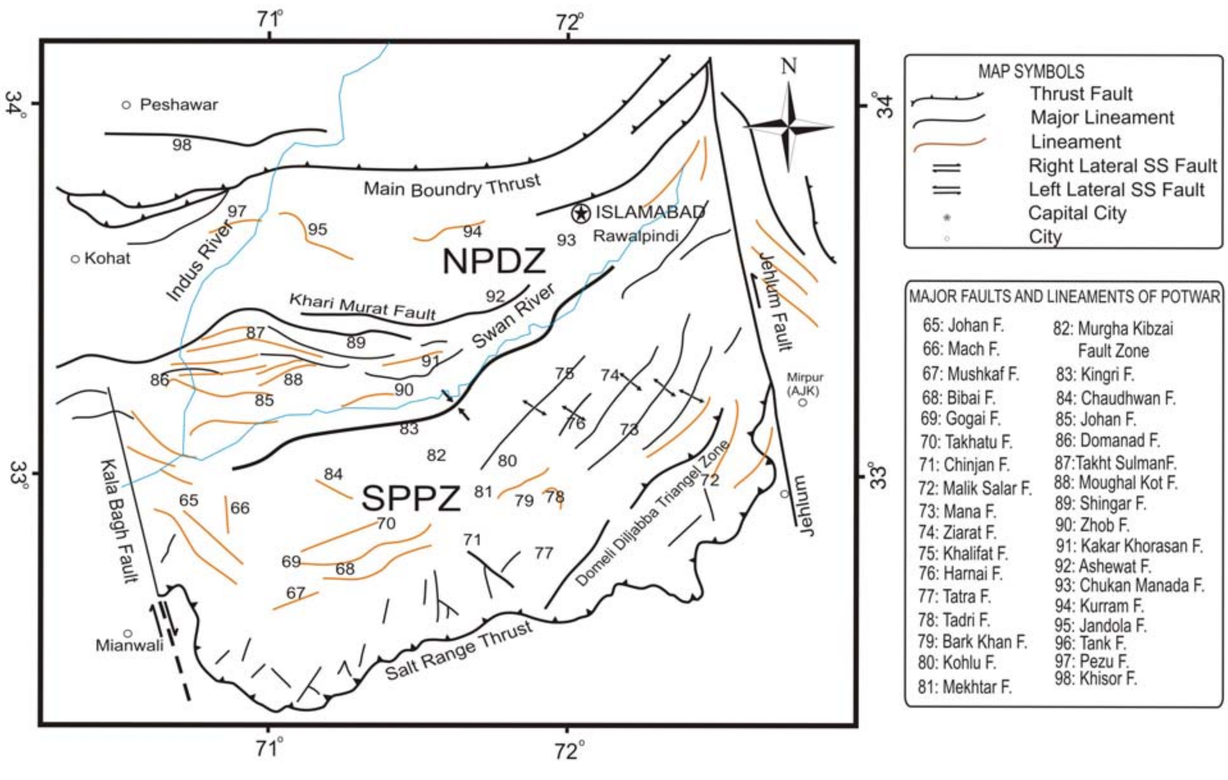

Figure 2 Tectonic map of the study area. The major tectonic subdivisions are clearly marked, i.e., the Northern Potwar Deformed Zone (NPDZ) and Southern Potwar Platform Zone (SPPZ).

2 Methodology

Remote sensing data is available in variety of formats and resolutions, and affects the quality of extracted geomorphic features. We used the SRTM DEM of 90 m resolution to extract drainage network and lineaments. The drainage network is extracted from digital elevation model of the area by calculating flow directions at all points using D8 algorithm. Flow direction is dependent on upslope area and specific catchment area, so both are calculated efficiently. The choice of stream delineation algorithms can influence the stream parameters like contributing area, slope, elevation, downstream distance and Strahler order. Stream longitudinal profiles are identified and selected based on least cost path analysis that computes the paths of least resistance down slope (i.e. the downstream flow path). Individual streams are prepared in ASCII format for further processes. As the extracted streams contain some error, so some smoothening algorithms are applied depending upon number of node, i.e., smoothing factor. This algorithm was implemented in MATLAB and calculated all the required parameters. Stream profile analysis was applied on each stream to obtain valuable information based on bedrock incision model which states that detachment limited channels did not observe a continuous cover of alluvial sediments, even at low flow because of equal stream gradient for erosion and uplift as shown in Figure 3.

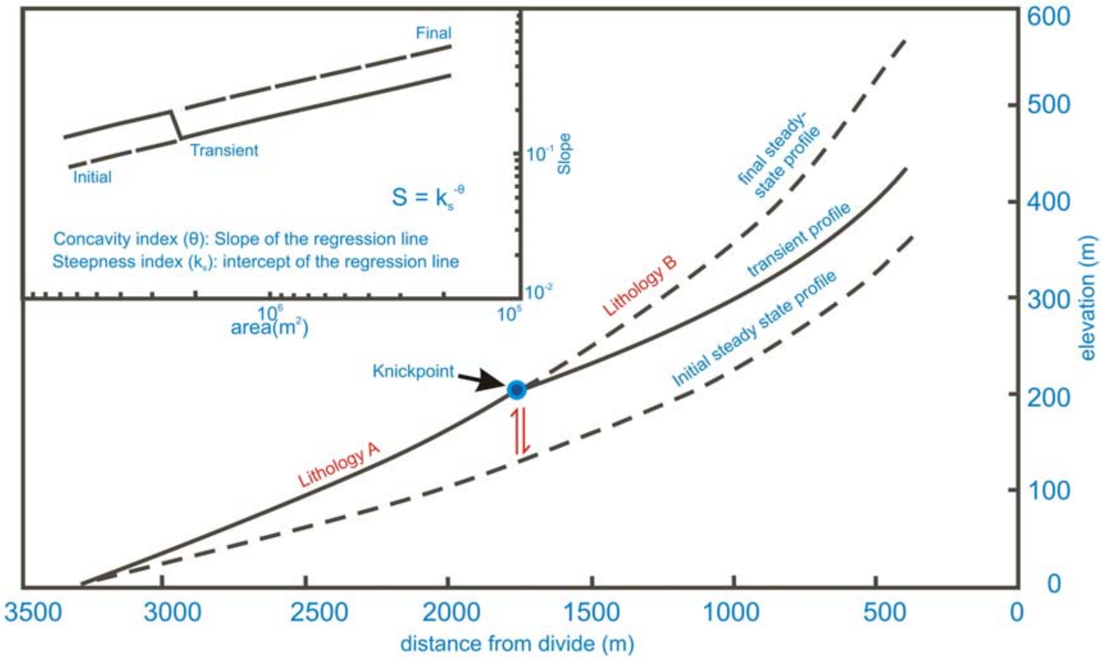

Figure 3 Transient-state profile between initial low-uplift and final high-uplift zones. The knick zone which is represented by knickpoints migrates upstream as the channel responds to the uplift-rate change. This migration is dependent upon the lithology of both units and/or fault activity. The inset shows the slope vs. drainage area data for the longitudinal profiles in which the channel concavity θ is the same for both the initial and final profiles, while the steepness, k_s, is considerably higher for the final profile. This figure is modified from that of Snyder et al. (2000).

The contrasts in lithologies or presence of faults help the streams to reach a new equilibrium condition. Mathematically, this can be written in following form:

$$\frac{dz}{dt} = U - E = U - KA^m S^n \quad (1)$$

where U and E represent uplift and erosion rates, respectively. K represents erosion efficiency factor which is directly related to sediments and rock strength, A is upstream drainage area and S is channel slope. The constants m and n are dependent on basin hydrology, hydraulic geometry and erosion process. dz/dt represents the changing rate of elevation with respect to time and if landscape is in steady-state condition, then it is equal to 0. Thus for a steady state landscape, equation 1 can be written as:

$$S = \left(\frac{U}{K}\right)^{1/n} A^{m/n} \qquad (2)$$

where m/n shows the concavity of the profile and coefficient $(U/K)^{1/n}$ is steepness of the profile. Power function for stream gradients is represented by

$$S = k_s A^{-\theta} \qquad (3)$$

where θ and k_s are concavity and steepness indices, respectively. They can be measured directly by regression analysis of data as shown in equation 3, i.e., area and slope (Howard 1994, Montgomery et al. 1996, Schoenbohm et al. 2004, Snyder et al. 2000, Whipple 2004, Wobus et al. 2006). By combining equations 2 and 3 we can get a useful relationship for calculating uplift rates.

$$U = k_{sn}{}^{n} K \qquad (4)$$

where k_{sn} is normalized steepness index. This equation gives us uplift rate for the area with steady state landscape by choosing appropriate values of m, n and K. Stream profile analysis is implemented on the selected trends of each stream for calculating channel parameters. Geomorphic parameters, i.e., concavity and steepness values are calculated after logarithmic regression analysis of area and slope values of a selected trend. The mean concavity index is calculated by using the concavity index of upper segment of each stream. Normalized steepness index is calculated using this mean concavity or a regionally estimated concavity index. The uplift rate as shown in equation 4 is a function of normalized steepness index k_{sn}, constants n and K. We can calculate the uplift rates in the area by assuming constant values of n and K which can be obtained from already available studies (Anderson et al. 1994, Seidl and Dietrich 1992, Tucker and Slingerland 1996, Wobus et al. 2006). Knickpoints are important tool to understand the landscape response to a base level fall and the corresponding sediment fluxes from rejuvenated catchments. We identified those points on individual stream profiles and hence their spatial distribution is available in map view to see the tectonic behavior (Bishop et al. 2005).

We prepared the lineament database of the area using Hough transformation to study this relationship (Gloaguen et al. 2007). We calculated the attitude of these extracted lineaments and streams of the drainage network. We prepared the rose diagrams of the lineaments and drainage network to observe their inter-relationship. In order to perform the detailed analysis we calculated the correlation between the drainage network and lineaments because we still did not know the quantitative relationship between flow directions of rivers and fault alignment. This correlation could help us understand the influence of lineaments on the drainage or vice versa. For this reason we compared the local correlation between DEM extracted lineaments and drainage network of the area respectively. To calculate these parameter two different line systems A_1 and A_2 are to be considered:

A_1 = Drainage system

A_2 = Lineaments system

The line densities (intensities) λ_1 and λ_2 of these two systems are measured first:

$$\lambda_1 = \left[\frac{length(A_1)}{Area}\right] \qquad (5)$$

where length (A_1) is the total line length of the drainage system and line density is measured in inverse of distance, i.e., $[\mathrm{Km}]^{-1}$. The reduced covariance C_{12} gives the expected total line length of A_2 measured in a circle with radius r. The circle is placed at any point belonging to A_1. The C_{12} is well approximated by moving the circle at regular intervals along A_2, measuring total fault lengths inside, and calculating the expected value over all measuring points. C_{12} completely describes the correlation between faults and streams (Clark and Wilson 1994, Grassberger and Procaccia 1983, Stoyan and Stoyan 1983).

$$G_{12}(r) = \left[\frac{\frac{d}{dr} C_{12}(r)}{2\pi r \lambda_2} \right] - 1 \qquad (6)$$

G_{12} is a local correlation coefficient and is a function of radius r. We plotted these computed values of G_{12} vs. r and connected the points. This graph shows us the influence of drainage system over the lineaments and vice versa.

3 Results and Discussions

The principle goal of tectonogeomorphology is to extract tectonic information from the longitudinal profiles. These profiles contain tectonic information in the form of knickpoints and their Strahler order as well. In any profile the knickpoints migrates upstream or downstream as the channel responds to the tectonic changes or the change of the lithology along the path of the stream. These stream profiles show the difference between initial low-uplift and final high-uplift zone as shown in Figure 3. By using stream power law the data obtained for steepness and concavity indices mostly give similar information, because a downstream transition between two different steepness values is normally bridged by a zone of very high or low concavity. However the channel concavity θ remains the same for both the initial and final profiles, while the steepness, k_s, becomes considerably higher for the final profile (Snyder et al. 2000). In other words, the general low concavities of streams indicate downstream increases in either incision rate or change in rock strength. The sharpness of the knickpoints gives relative information that how the more recent tectonics or river capture events had occurred. In general, the sharper the knickpoints, the more recently it developed (Wobus et al. 2006).

We have studied the Swan River which bisects the Potwar Plateau into two parts. The extracted streams and lineaments are located on both sides of the river as shown in Figure 8. We have studied all the streams and main channel by stream power law. The analysis of three prominent streams, i.e., Main Swan River, Stream A in NPDZ and Stream B in SPPZ is discussed here in details. Figure 4 shows the stream profile analysis of the Swan River. This is a three segment channel and represents relict landscape. The presence of active tectonic features is observed with the help of two knickpoints. The first knickpoint shows the presence of Main Boundary thrust while the second point is right after the end of the Rawal Lake which is another import geomorphic feature in the vicinity of Islamabad along Murree Road. This profile observes three trends based on the morphological observation, i.e., an upper segment, middle segment and lower segment. The upper segment travels over relict landscape with low steepness index 70.1 and uniform concavity index 0.31, which mean that they have been less eroded during the recent erosion processes. The middle segment shows intermediate concavity 1.75 and steepness 56.63, which shows that the area has undergone intermediate erosion process or uplift. The lower segment suggests higher concavity and lower steepness indices, i.e., 2.71 and 36.2. Along the downstream of the river, the sudden change in the geomorphic indices shows gradual change in lithology and tectonic activity. The eastern section of the river has high steepness values and because steepness is directly proportional to uplift rate it means that we have more deformation processes working on eastern section as compared to central or western section. Previous studies also suggest that the eastern section is more deformed and this deformation decreases towards central and western section of the plateau (Moghal et al. 2003). We studied streams A and B from NPDZ and SPPZ, respectively to understand the lineament behavior, shown in Figure 5 and 6. The morphology of both streams consists of two segments with identified knickpoints. The first segment of Stream A shows relict landscape with no or very little erosion, but after crossing the Khairi Murat Fault it shows high concavity and steepness indices. Stream B is flowing in SPPZ and has higher concavity values from 0.99 to 1.08. But both segments have almost equal values of steepness index of 9.8 and 9.5 which are generally very low. As the values of steepness are directly related to uplift, thus comparing these values to those of Stream A we can conclude that NPDZ is more deformed and is uplifting, while SPPZ is more stable. The detailed concavity and steepness values are shown in Table. This table shows increasing normalized steepness and concavity from the upper, middle to lower segments, and high variability of concavity indices in the middle segments and normalized steepness indices in the upper segment. The normalized steepness index is calculated with a fixed mean concavity value of 0.45.

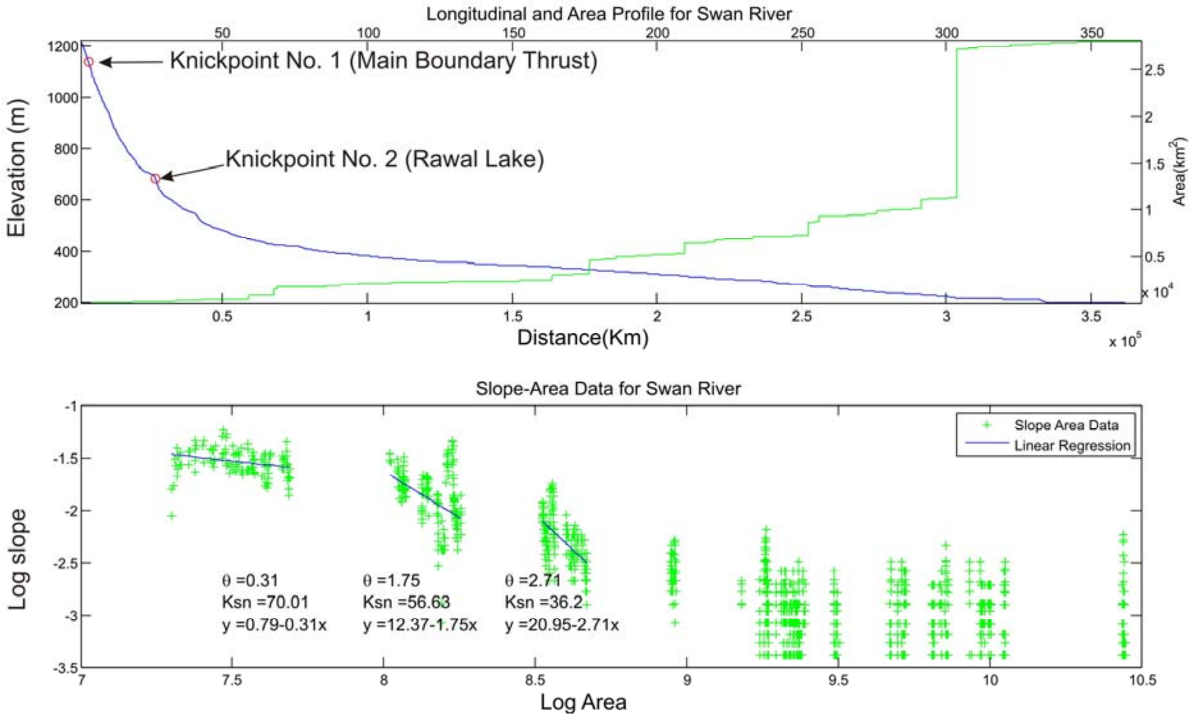

Figure 4 Stream profile analysis of the Swan River. It clearly shows that the two main knickpoints and three clear segments are identified. This helps us separate the Eastern, Western and Central Potwar.

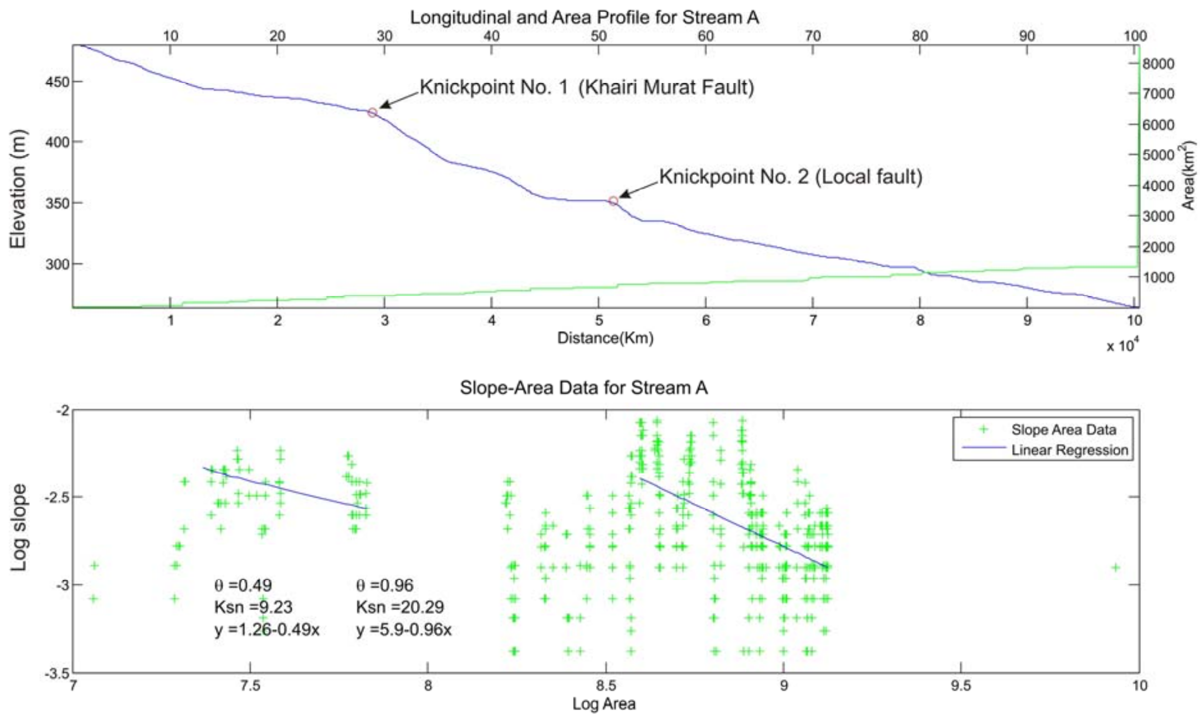

Figure 5 Stream profile analysis of Stream A from NPDZ. It clearly shows that the location of Khairi Murat Fault is identified by the two main knickpoints.

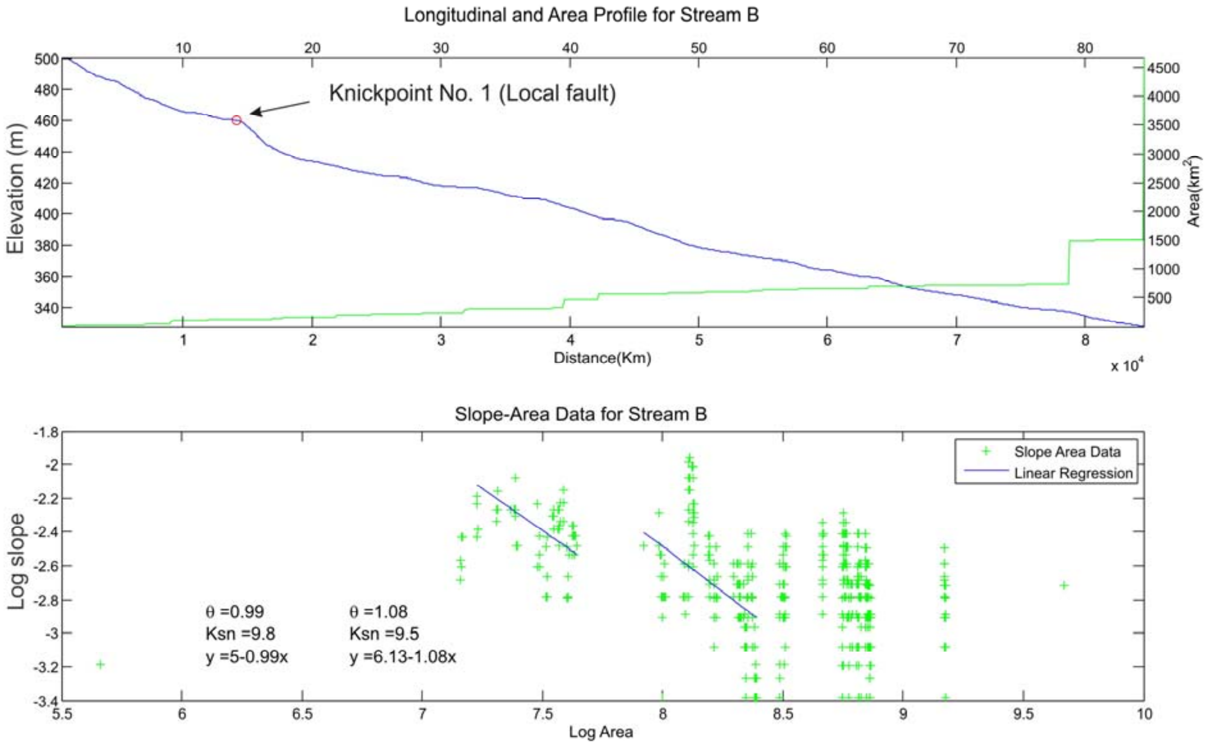

Figure 6 Stream profile analysis of Stream B from SPPZ. It is a two segment profile showing very less variation in steepness.

Table 1 Normalized steepness and concavity values

	Total stream No.	Concavity	Normalized steepness
Upper segment	79	0.82212 ± 0.62575	16.2807 ± 9.9173
Middle Segment	18	2.0587 ± 1.0809	20.2293 ± 11.3447
Lower Segment	2	2.8607 ± 0.21998	28.3245 ± 11.1383

We apply stream profile analysis on all the 112 streams of the extracted drainage network, and calculate the concavity and steepness values. By using these concavity and steepness values we calculate the uplift rates in different areas of the plateau and try to correlate them to the ongoing deformation processes. The determination of uplift rates with stream profile analysis is based on assumptions, mainly with regard to the steady-state incision process. The uplift rate map of the area is shown in Figure 7. The uplift rate map shows the amount of uplift per year in different parts of the plateau. In the eastern section the uplift rate ranges from 0.0041 cm/yr to 0.070 cm/yr, in the central section from 0.016 to 0.025 cm/yr and in the western section from 0.004 to 0.01 cm/yr. This suggests that the eastern section has been experiencing more uplift compared to the rest of the plateau.

We then compare lineaments and drainage network and try to figure out their influence on each other, but the visual interpretation is not enough to provide sufficient information due to structural complexity of the Potwar Plateau. The local correlation provides the interrelationship between streams and faults. It is especially a means of preliminary graphical exploratory investigation that enables the user to quickly estimate in how far streams are affected by active tectonic processes. The extracted drainage network and lineaments are

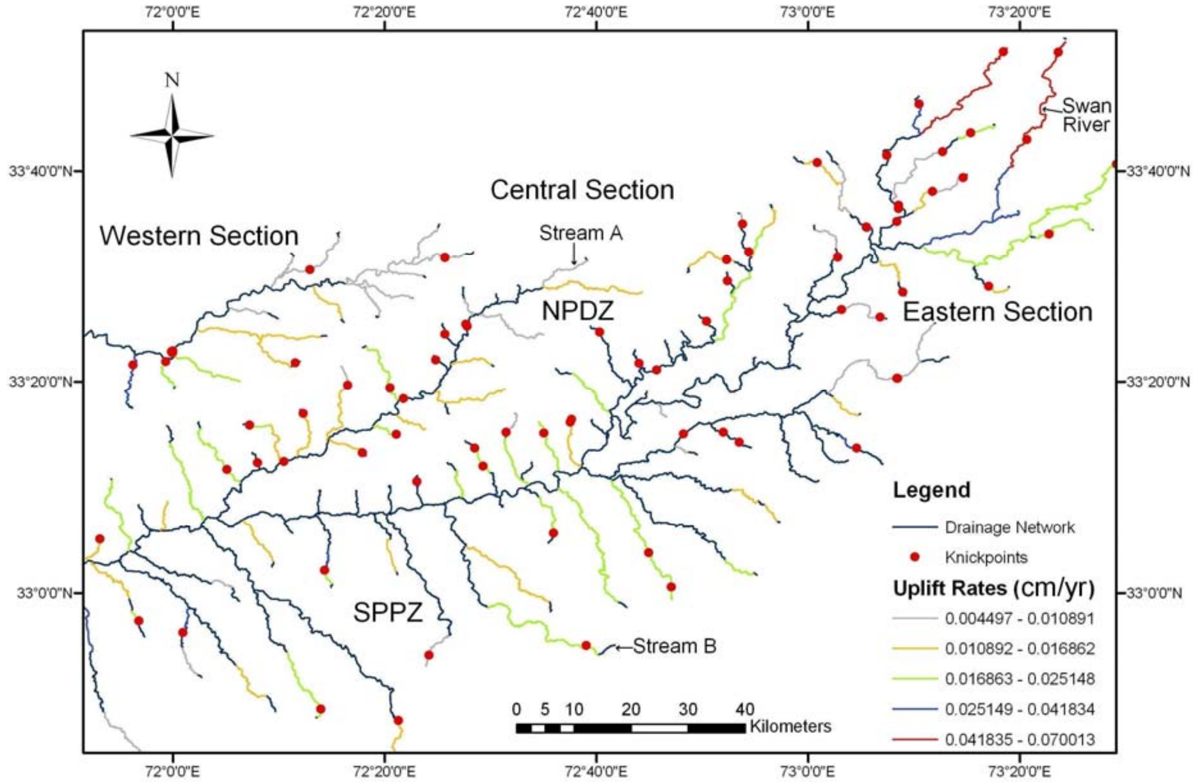

Figure 7 Uplift rate map of the area showing uplift values (cm/yr). Distribution of the uplift rates and knickpoints helps us not only quantify the amount of deformation, but also separate eastern, central and western sections.

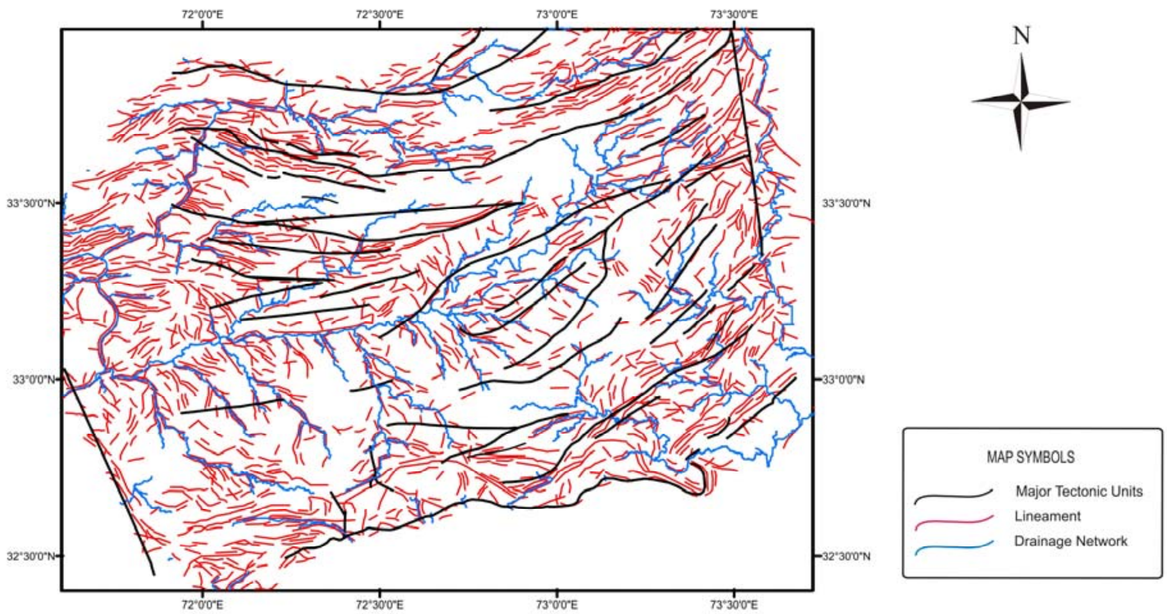

Figure 8 Lineaments and drainage network map. These are extracted from DEM.

also shown in Figure 8. We calculate the local correlation between drainage and lineaments using equations 5 and 6. The local correlation is shown in Figure 9. These results show that the flow of streams and their orientation are affected by lineaments within the range of 1 km. So in more deformed area they are very much close to each other and drainage pattern is more dendrite as it is in the case of the eastern section of this plateau. The localized lineaments have their play in developing the shape of the local drainage though they are also controlled by major tectonic elements as shown in Figure 8.

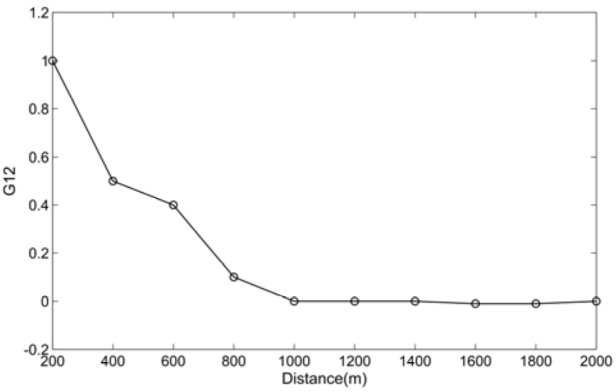

Figure 9 Local correlation based upon drainage network and lineaments extracted from DEM

River profile analysis uses assumption of steady state condition but in spite of this drawback it remains a powerful qualitative tool. This analysis gives important indications on the undergoing tectonic processes even though the fluvial incision processes are not fully understood. This holds true, especially if the slope-area data are assessed in the context with other geological information at hand. In the case of the Potwar Plateau, the eastern section of strong deformation could be identified. Further, the distribution of relative uplift rates is inhomogeneous and is an evidence to suggest the existence of different sections with different relative uplift rates.

4 Conclusion

Digital elevation model (DEM) is a key component for computer-based analyses of river profiles and drainage basin extraction as it provides elevation information for the land surface throughout the catchment of the area. In this study we applied tectonogeomorphological analysis on the Swan River to study its behavior. The change in the course of this river is mainly due to tectonics and the subsurface lithology of the area. The drainage network of the area continues to develop with the change of tectonics in this region. This study can be improved by using high resolution DEMs/GPS data and other geological information. The uplift rate map of the area shows high uplift in the northern Potwar deformed zone. Due to the structural complexity it is very important to measure the influence of streams and lineaments on each other. The local correlation suggests that the lineaments and streams of the area interact with each other and influence their orientation and style. The main source of this influence is thin skinned tectonics of the area.

Acknowledgements

Authors wish to thank Prof. YU Dafu for careful comments which improve the quality of the manuscript. The Financial assistance to Faisal Shahzad from Saxony Government, Germany is gratefully acknowledged.

References

Anderson, R. S., G. S. Dick, and A. Densmore. 1994. Sediment Fluxes from Model and Real Bedrock-channeled Catchments: Responses to Baselevel, Knickpoint and Channel Network Evolution. Geological Society of America Abstracts With Programs **26**:238-239.

Baker, D. M., R. J. Lillie, R. S. Yeats, G. D. Johnson, M. Yousuf, and A. S. H. Zamin. 1988. Development of the Himalayan Frontal Thrust Zone: Salt Range, Pakistan. Geology **16**: 3-7.

Bishop, P., T. B. Hoey, J. D. Jansen, and I. Lexartza Artza. 2005. Knickpoint Recession Rate and Catchment Area: The Case of Uplifted Rivers in Eastern Scotland: Earth Surface Processes and Landforms **30**: 767-778.

Clark., C. D., and C. Wilson. 1994. Spatial Analysis of Lineaments. Computer and Geosciences **29**: 1237-1258.

Gloaguen, R., P. R. Marpu, and I. Niemeyer. 2007. Automatic extraction of Faults and Fractal Analysis from Remote Sensing Data. Nonlinear Processes in Geophysics **14**: 131-138.
Grassberger, P., and I. Procaccia. 1983. Measuring the strangeness of strange attractors: Phyisca 9D, p. 189-208.
Howard, A. D. 1994. A Detachment-limited Model of Drainage Basin Evolution. Water Resources Research **30**: 2261-2285.
Jadoon, I. A. K., and W. Frisch. 1997. Hinterland-vergent Tectonic Wedge below the Riwat Thrust, Himalayan Foreland, Pakistan: Implications for hydrocarbon exploration. American Association of Petroleum Geologists Bulletin **81**: 438-448.
Jadoon, I. A. K., W. Frisch, A. Kemal, and T. M. Jaswal. 1997. Thrust Geometries and Kinematics in the Himalayan Foreland (North Potwar deformed zone), North Pakistan. Geologische Rundschau**86**: 120-131.
Jan, M. Q., M. Gaetani, and A. Zanchi. 2005. 32nd International Geological Congress Field Trip (PR01): A Traverse through Himalaya-Karakorum of Pakistan. Episodes **28**: 124-125.
Kazmi, A. H., and M. Q. Jan. 1997. Geology and Tectonics of Pakistan, Graphic Publishers. Karachi.
Khan, M. A., R. Ahmed, H. A. Raza, and A. Kemal. 1986. Geology of Petroleum in Kohat-Potwar Depression, Pakistan. American Association of Petroleum Geologists Bulletin **70**: 396-414.
Moghal, M. A., A. Hameed, M. I. Saqi, and M. N. Bugti, 2003, Subsurface Geometry of Potwar Sub-Basin in relation to Structuration and Entrapment: SPE- Annual Technical Conference and Oil show 2003-Islamabad, Pakistan.
Monalisa, Khwaja A.A., and M. Qaiser. 2002. Focal Mechanism Studies of Kohat and Northern Potwar Deformed Zone. Geo.l Bul. Univ. of Peshawar **35**: 85-95.
Monalisa, A. A. Khwaja, and M. Q. Jan. 2007. Seismic Hazard Assessment of the NW Himalayan Fold-and-thrust Belt, Pakistan, Using Probabilistic Approach. Journal of Earthquake Engineering **11**: 257-301.
Montgomery, D. R., T. B. Abbe, J. M. Buffington, N. P. Peterson, K. M. Schmidt, and J. D. Stock. 1996. Distribution of Bedrock and Alluvial Channels in Forested Mountain Drainage Basins. Nature **381**: 587-589.
Nakata, T., H. Tsutsumi, S. H. Khan., and R. D. Lawrence 1991. Active Faults of Pakistan, Map Sheets and Inventories, Research Center for Regional Geography, Hiroshima University, Japan.
O'Callaghan, J. F., and D. M. Mark. 1984. The Extraction of Drainage Networks from Digital Elevation Data. Computer Vision, Graphics, & Image Processing **28**: 323-344.
Pivnik, D. A., and N. A. Wells. 1996. The Transition from Tethys to the Himalaya as Recorded in Northwest Pakistan. GSA Bulletin **108**: 1295-1313.
Schoenbohm, L. M., K. X. Whipple, B. C. Burchfiel, and L. Chen. 2004. Geomorphic Constraints on Surface Uplift, Exhumation, and Plateau Growth in the Red River region, Yunnan Province, China. Bulletin of the Geological Society of America **116**: 895-909.
Seidl, M. A., and W. E. Dietrich. 1992. The Problem of Channel Erosion into Bedrock. Catena Supplement **23**:. 101-124.
Snyder, N. P., K. X. Whipple, G. E. Tucker, and D. J. Merritts. 2000. Landscape Response to Tectonic Forcing: Digital Elevation Model Analysis of Stream Profiles in the Mendocino Triple Junction Region, Northern California. Bulletin of the Geological Society of America **112**: 1250-1263.
Stoyan, D., and H. Stoyan. 1983. Quantifizierung Von Korrelationen Zwischen Geometrischen Strukturen auf geologischen Karten. Zeitschrift f¨ur angewandte Geologie **29**: 240-244.
Tucker, G. E., and R. Slingerland. 1996. Predicting Sediment Flux from Fold and Thrust Belts. Basin Research **8**: 329-349.
Whipple, K. X. 2004. Bedrock Rivers and the Geomorphology of Active Orogens. Annual Review of Earth and Planetary Sciences **32**: 151-185.
Wobus, C., K. Whipple, E. Kirby, N. Snyder, J. Johnson, K. Spyropolou, B. T. Crosby, and D. Sheehan, 2006, Tectonics from Topography: Procedures, Promise and Pitfalls, in S. D. Willett, N. Hovius, M. T. Brandon, and D. M. Fisher (eds.), Tectonics, Climate and Landscape Evolution, GSA Special Paper **398**, p. 55-74.